Appl. Phys. B
DOI 10.1007/s00340-013-5699-4

Applied Physics B
Lasers and Optics

Dynamics of blueshifted floating pulses in gas-filled hollow-core photonic crystal fibers

M. Facão · M. I. Carvalho

Received: 1 October 2013 / Accepted: 16 October 2013

Abstract Frequency blueshifting was recently observed in light pulses propagating on gas-filled hollow-core photonic crystal fibers where a plasma has been produced due to photoionization of the gas. One of the propagation models that is adequate to describe the actual experimental observations is here investigated. It is a nonlinear Schrödinger equation with an extra term, to which we applied a self-similar change of variables and found its accelerating solitons. As in other NLS-related models possessing accelerating solitons, there exist asymmetrical pulses that decay as they propagate in some parameter region that was here well defined.

1 Introduction

Hollow-core photonic crystal fibers (HC-PCF) have recently attracted a lot of attention particularly because they offer ultra-long single-mode interaction lengths for nonlinear optics in gaseous media [1]. Among the kind of HC-PCFs, we refer the kagomé type that was first reported in 2002 [2] and owes its name to the kagomé lattice cladding. The kagomé HC-PCF provides several hundred nanometers band of guidance at low loss levels (≈ 1 dB/m) and exhibits weak anomalous group velocity dispersion (GVD) over the entire transmission window, with low dispersion slope. Whenever filled with gas, it enables the self-compression of pulses to an extent that the peak intensities may attain values above the ionization threshold of the gas, allowing the production of a plasma. Then, the interaction of laser light with the plasma leads to new nonlinear effects such as the blueshifting [3] of the central wavelength of the pulse.

Recently, Saleh et al. [4, 5] presented an amenable model for describing the interaction between the optical pulse and plasma on those gas-filled kagomé HC-PCFs. The model was used by them to predict the extent of frequency blueshifting by means of a perturbation approach. Following these preliminary perturbation results, a thorough study on the existence of accelerating solitons to such a model, including the plasma but also the stimulated Raman scattering term, was performed [6]. There, it was shown that indeed there are self-similar pulse solutions of such model that accelerate while its central frequency blueshifts. However, it was reported that for large strength of the plasma nonlinearity or small pulse amplitudes, the pulses have distinguished long tails and decay as they propagate. The latter analysis was done with a scaling that resulted in a ODE with four parameters, one for the intensity threshold, other for the acceleration and both the plasma and Raman terms accommodated with only one parameter and a ratio between the strength of them. This scaling was such that both the extra nonlinear parameter and pulse amplitude of the final normalized model should be very small in order to describe the actual physical experiments. Here, we disregard the Raman term and use an approximate equation of this model that was already used in [4], and obtain a two-parameter ordinary differential equation (ODE) for the accelerating pulse profiles, finding the parameters ranges for symmetrical pulse profiles and for long tail pulses. Furthermore, our results, confirmed by numerical simulations of the evolution of

M. Facão (✉)
Departamento de Física, Universidade de Aveiro,
I3N, 3810-973 Aveiro, Portugal
e-mail: mfacao@ua.pt

M. I. Carvalho
DEEC/FEUP, INESC TEC, Universidade do Porto,
Rua Dr. Roberto Frias, 4200-465 Porto, Portugal

Published online: 27 October 2013

sech pulses, also show that even though there is always pulse decay for the parameter range corresponding to asymmetrical pulse profiles, the decay rate can increase or decrease during propagation depending on these parameters.

2 One-parameter ODE and perturbation approach

The model introduced in [4, 5] for pulse propagation in nonlinear gaseous media presenting Kerr and plasma nonlinearities has the following dimensionless version

$$i\frac{\partial q}{\partial \xi}+\frac{1}{2}\frac{\partial^2 q}{\partial \tau^2}+|q|^2 q-\phi_T q\left(1-\mathrm{e}^{-\sigma\int_{-\infty}^{\tau}\Delta|q|^2\Theta(\Delta|q|^2)d\tau'}\right)=0 \tag{1}$$

where $q=(\gamma z_0)^{1/2}\psi$ represents the optical field envelope ψ, $\xi=Z/z_0$ and $\tau=t/t_0$ are normalized versions of the propagation distance Z and time t in a reference frame that travels at group velocity, $\phi_T=\frac{1}{2}k_0 z_0(\omega_T/\omega_0)^2$ refers to the maximum plasma frequency ω_T and $\sigma=\tilde{\sigma}t_0/(A_{\mathrm{eff}}\gamma z_0)$ to the photoionization cross section $\tilde{\sigma}$, $\Delta|q|^2=|q|^2-|q|^2_{\mathrm{th}}$ where $|q|^2_{\mathrm{th}}$ is related to the ionization intensity threshold and Θ is the Heaviside step function. On these latter relations, $z_0=t_0^2/|\beta_2|$ is the so-called dispersion length (β_2 is the GVD parameter), t_0 is an arbitrary time chosen similar to the pulse duration, A_{eff} is the effective optical mode area, γ is the nonlinear Kerr parameter, ω_0 is the central frequency of the pulse and k_0 the corresponding vacuum wavenumber. Note that this model assumes that the recombination time is longer than the pulse and does not consider the ionization-induced loss that is small especially for pulses whose peak is barely above the threshold.

Referring to experimental data [3], we arrived to values of σ around 10^{-4} and values for q and q_{th} around the unity. Hence, the exponential term may be approximated by a two-term Maclaurin expansion giving

$$i\frac{\partial q}{\partial \xi}+\frac{1}{2}\frac{\partial^2 q}{\partial \tau^2}+|q|^2 q-\eta q\int_{-\infty}^{\tau}\Delta|q|^2\Theta(\Delta|q|^2)d\tau'=0 \tag{2}$$

where $\eta=\sigma\phi_T$. Applying the same accelerating variable as in [6], namely, $T=\tau+\frac{a}{4}\xi^2+b\xi$ and $q(\xi,\tau)=F(T)\exp(i\theta(\xi,T))$, with F and θ real, we obtain the ODE for F

$$F''+\left(aT-D+2F^2-2\eta\int_{-\infty}^{T}\Delta F^2\Theta(\Delta F^2)dT'\right)F=0$$

and the phase

$$\theta(\xi,T)=-\left(\frac{a}{2}\xi+b\right)T+\frac{1}{2}(D+b^2)\xi+\frac{1}{4}ba\xi^2+\frac{1}{24}a^2\xi^3+E. \tag{3}$$

In this case, the ODE for the pulse profile may be further simplified if one uses the following change of variables

$$F(T)=\frac{2\eta}{\beta}P(\zeta),\quad \zeta=\frac{2\eta}{\beta}T,$$

obtaining

$$P''+\left(\beta\zeta-G+2P^2-\beta\int_{-\infty}^{\zeta}\Delta P^2\Theta(\Delta P^2)d\zeta'\right)P=0, \tag{4}$$

where a and η were replaced by the single parameter $\beta=(8\eta^3/a)^{1/2}$ and $G=(\beta/2\eta)^2 D$ is the new constant.

As the evolution Eq. (2) is the nonlinear Schrödinger equation (NLSE) with the extra term representing the plasma–light interaction, sech soliton solutions may be anticipated for the ODE (4) with $\beta=0$. In fact, these sech solutions are of the form $P_0(\zeta)=\sqrt{G}\,\mathrm{sech}\left[\sqrt{G}(\zeta-\zeta_0)\right]$. Hence, let us write an expansion for $P(\zeta)$ in the form

$$P(\zeta)=P_0(\zeta)+\beta P_1(\zeta)+\cdots$$

and introduce it into (4) which yields

$$P_1''+(-G+6P_0^2)P_1=-\zeta P_0+P_0\int_{-\infty}^{\zeta}(P_0^2-P_{\mathrm{th}}^2)\times\Theta(P_0^2-P_{\mathrm{th}}^2)d\zeta'$$

The homogeneous part of the above equation is satisfied by P_0' so that the solvability condition is

$$\int_{-\infty}^{\infty}\left(-\zeta P_0P_0'+P_0P_0'\int_{-\infty}^{\zeta}(P_0^2-P_{\mathrm{th}}^2)\Theta(P_0^2-P_{\mathrm{th}}^2)d\zeta'\right)d\zeta=0,$$

which gives the following algebraic equation for the amplitude squared, G, of the zero-order soliton solution

$$G=\frac{3}{2}\left(1-\frac{P_{\mathrm{th}}^2}{G}\right)^{-3/2}. \tag{5}$$

As long as β is relatively small, we may say that the peak amplitude of q is $|q|_{\mathrm{peak}}=\frac{2\eta}{\beta}\sqrt{G}$, which implies that the acceleration parameter is $a=\frac{2\eta}{G}|q|^2_{\mathrm{peak}}$ and the frequency shift becomes $\Delta\omega=-\frac{d\theta}{dT}=\frac{\eta}{G}|q|^2_{\mathrm{peak}}\xi$. Note that in case the intensity threshold is zero, the Eq. (5) may be exactly solved to $G=3/2$, which gives $a=\frac{4\eta}{3}|q|^2_{\mathrm{peak}}$ and

$\Delta\omega = \frac{2\eta}{3}|q|^2_{\text{peak}}\xi$, indicating that the blueshift is proportional to the square of the peak amplitude [4]. On the other hand, for finite $|q|_{\text{th}}$, the use of (5) allows us to write $a = \frac{4\eta}{3|q|_{\text{peak}}}\left(|q|^2_{\text{peak}} - |q|^2_{\text{th}}\right)^{3/2}$ and $\Delta\omega = \frac{2\eta}{3q|_{\text{peak}}}\left(|q|^2_{\text{peak}} - |q|^2_{\text{th}}\right)^{3/2}\xi$, expressions that clearly show that the actual dependence of the blueshift process on the peak amplitude is more complex, with both the pulse peak amplitude and the threshold intensity playing an important role in it [6].

3 Pulse profiles

The pulse solutions to ODE (4) were obtained using a shooting method that relied on Airy function asymptotics and first estimates coming from the above perturbation approach. In fact, at the tails, the Eq. (4) reduces to

$$P'' + (\beta\zeta - G - \beta\Lambda_\infty)P = 0,$$

where $\Lambda_\infty = 0$ if $\zeta \to -\infty$ and $\Lambda_\infty = \int_{-\infty}^{\infty} \Delta P^2 \Theta(\Delta P^2) d\zeta'$ if $\zeta \to \infty$, which is equivalent to an Airy equation by the following change of variables $z = -\beta^{1/3}(\zeta - \Lambda_\infty) + \beta^{-2/3}G$. Hence, the asymptotics of the pulses conform with Airy functions, particularly, they match the Ai(z) at the left tail and Bi(z) at the right tail since these are the exponentially decaying Airy solutions at $z \to \infty$ and $z \to 0^+$, respectively. Note that this is true as long as z is in the positive semi-axis.

The analysis up to this stage may seem very similar to the analysis applied to the more general Eq. (1) in [6]. Also, the results obtained there could possibly predict the profile characteristics of pulse solutions of (2); however, the shooting calculations with the ODE obtained in [6] and small values of peak amplitudes and plasma strengths would involve Airy function values for large arguments that are not easily evaluated. Moreover, the present ODE is, for each P_{th}, a one-parameter ODE; thus, we may obtain all the amplitudes and accelerations with one run that spans a considerable range of β. The acceleration results for two of these runs are shown in Fig. 1. Regarding the pulse profile characteristics, our results confirm that the asymmetry will happen for small peak amplitudes or large plasma term strength. The long right tails that characterize the asymmetry of these pulses are related to the ζ location of the pulse, namely long tails are expected if ζ_0 is such that the corresponding z of the Airy equation is close to zero. In such cases, the asymptotics at the right tail cannot be exponentially since, at $z<0$, Bi(z) is no longer exponentially decaying but instead both Bi and Ai are algebraically decaying functions. In order to visualize the ranges of peak amplitude, threshold amplitude and η values

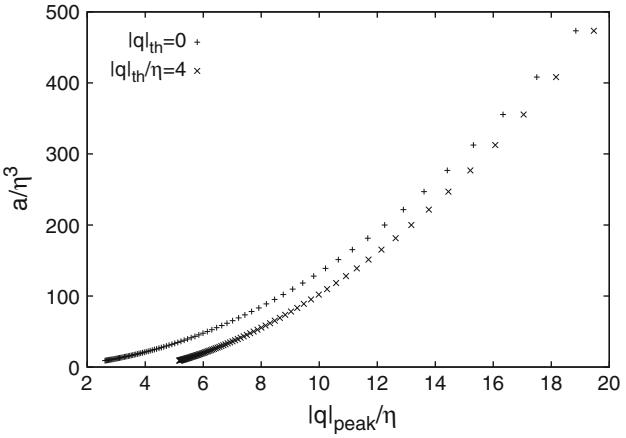

Fig. 1 Dependence of acceleration parameter on the pulse peak amplitude, normalized by η^3 and η, respectively, for $|q|_{\text{th}} = 0$ and $|q|_{\text{th}}/\eta = 4$

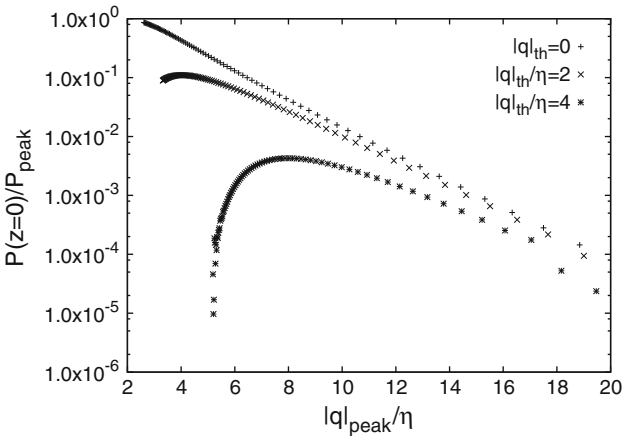

Fig. 2 Ratio $P(z = 0)/P_{\text{peak}}$ against $|q|_{\text{peak}}/\eta$ for several $|q|_{\text{th}}$

for which the long tails exist, we have plotted the ratio of the value of P at $\zeta(z = 0)$ to P_{peak} against $|q|_{\text{peak}}/\eta$ for several $|q|_{\text{th}}$ (Fig. 2). The larger this ratio is, the closer to $z = 0$ is the pulse location, and thus the longer are the right tails and the asymmetry. The analysis of results presented in Fig. 2 shows that for $q_{\text{th}} = 0$, the long tails happen for small $|q|_{\text{peak}}/\eta$, achievable with small peak amplitudes and relatively large plasma strength (recall that we are dealing with an approximation of the initial model that is valid for small plasma term). In the more realistic case of $q_{\text{th}} \neq 0$, the long tails happen in the same conditions with the exception that the profile is closest to the Airy $z = 0$ for some small finite $|q|_{\text{peak}}/\eta$.

In order to assess how the existence of such long tails would be perceived in a real experiment, we decided to numerically investigate the propagation of a fundamental soliton with peak amplitude and duration similar to the ones that have allowed the experimental observation of

the blueshift effect [3]. For this purpose, Eq. (2) was solved using the values presented in Saleh et al. [4] ($I_{\text{th}} \simeq 64$ TW/cm^2 and $\tilde{\sigma} = 1.03 \times 10^{-3}$ cm^2 Hz/W) and other parameters from Hölzer et al. [3]. For a pulse with $\lambda = 800$ nm at the maximum compression width of 2.5 fs propagating in 1.7 bar Argon-filled kagomé PCF whose $\beta_2 = -7.5 \times 10^{-28}$ s^2/m and $\gamma = 2.7 \times 10^{-7}$ W^{-1} m^{-1} ($n_2 = 1.8 \times 10^{-23}$ m$^2/W$ from [7]), we obtain $\sigma = 2.15 \times 10^{-4}$, $\phi_T = 8.26 \times 10^2$ which gives $\eta = 0.18$, $q_{\text{th}} = 0.88$ and $|q|_{\text{th}}/\eta = 4.9$. Hence, in this case, the maximum value of $P(z = 0)/P_{\text{peak}}$ is very small (smaller than 0.01) and the respective pulse profiles should be symmetric and propagate without radiation shedding, which is confirmed by the direct simulation of (2) for $|q|_{\text{peak}} = 1.12$ and $\xi = 40$ (corresponding to 34 cm) that is shown in Fig. 3. On the other hand, we envisage an experiment in the same fiber and same pulse width but for a pump wavelength of 1.064 μm that would give $\eta = 0.35$, $q_{\text{th}} = 0.45$ and $q_{\text{th}}/\eta = 1.27$. In this case, Fig. 2 suggests that pulses with small peak amplitudes should exhibit a long right tail and decay as they propagate, as may be confirmed by the direct simulation of a fundamental soliton with peak amplitude $|q|_{\text{peak}} = 0.69$ for $\xi = 102$ (also corresponding to 34 cm) shown in Fig. 4. In effect, this pulse is also propagating along a parabolic trajectory, but during propagation, several humps from the right tail become visible. The pulse decay is more clearly seen in Fig. 5, which compares the evolution of the pulses peak amplitude, normalized to their input value, for the two cases considered. In effect, while the curve for the first case exhibits small amplitude oscillations around a constant value, in the second case, the oscillations have a considerable amplitude in the beginning, decreasing afterward, but, more importantly, the peak mean value is decreasing during propagation. This behavior can be explained by the fact that the stationary profile of the pulse corresponding to the parameters considered in Fig. 4 has a significant left tail that carries infinite energy due to its Airy algebraic decay. As the input pulse evolves toward this stationary profile, its peak will naturally decrease in order to feed the tail that is forming. The difference in the two cases considered in Figs. 3 and 4 was just a change in the pump wavelength that decreased the ratio $|q|_{\text{th}}/\eta$ and increased η, both contributing for the observation of long tails and pulse decay. However, other physical parameters, such as the gas pressure and the fiber geometry, may change the accelerating pulse profile characteristics imposing or not pulse decay during propagation. The amplitude oscillations, observed in both cases, do not have a constant period but their average period does increase with $\beta^{8/3}/\eta^2$ as may be obtained by a simple analysis of the spectral stability problem [8], namely, the oscillation period should be close to the value of the edge of the continuous spectrum and that edge is, in this problem, varying with $\beta^{8/3}/\eta^2$.

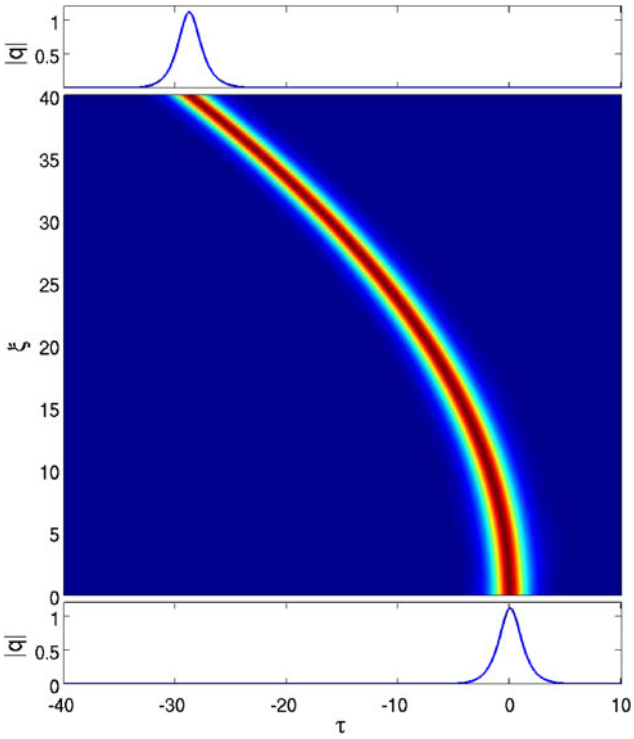

Fig. 3 Pulse evolution for $|q|_{\text{peak}} = 1.12$, $\eta = 0.18$ and $q_{\text{th}} = 0.88$

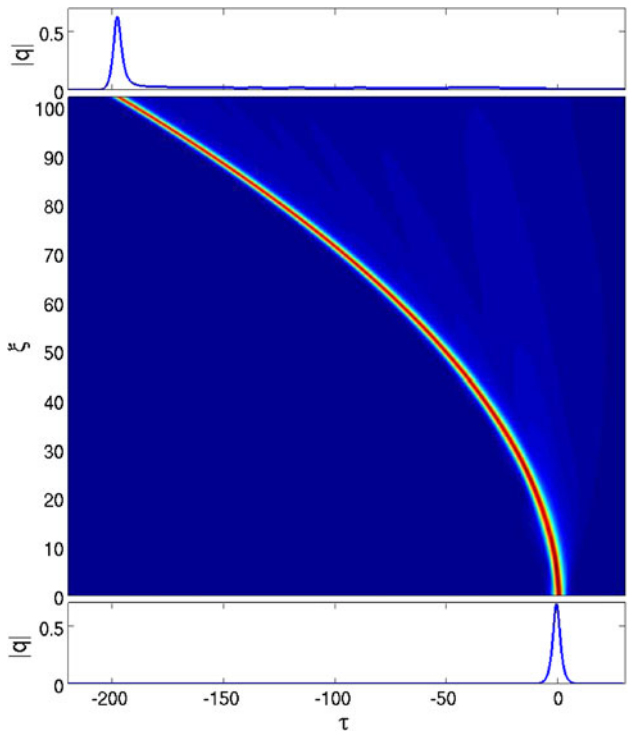

Fig. 4 Pulse evolution for $|q|_{\text{peak}} = 0.69$, $\eta = 0.35$ and $q_{\text{th}} = 0.45$

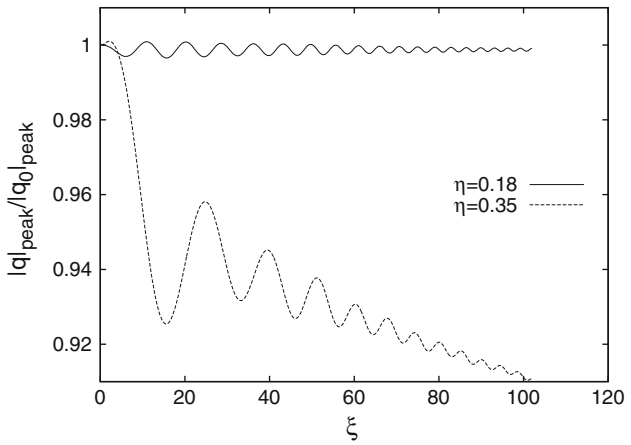

Fig. 5 Peak amplitude evolution for $|q|_{\text{peak}} = 1.12$, $\eta = 0.18$ and $q_{\text{th}} = 0.88$ ($\beta = 0.78$) and for $|q|_{\text{peak}} = 0.69$, $\eta = 0.35$ and $q_{\text{th}} = 0.45$ ($\beta = 1.9$)

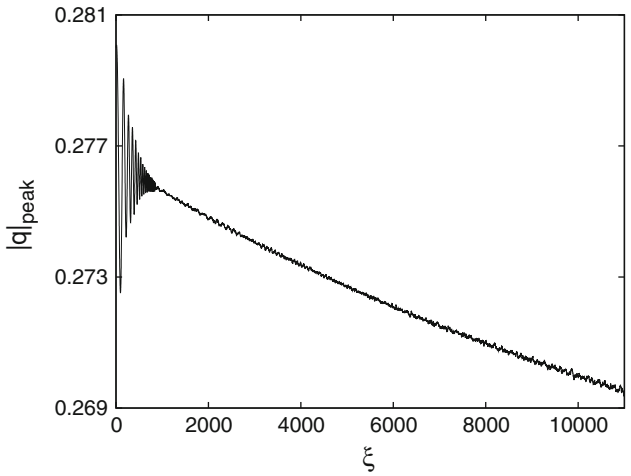

Fig. 6 Peak amplitude evolution for $|q|_{\text{peak}} = 0.28$, $\eta = 0.1$ and $q_{\text{th}} = 0.2$ ($\beta = 1.5$)

Returning to the dynamics of the decaying pulses, let us note that since the peak amplitude decreases, the corresponding stationary profile is also varying. In the case $q_{\text{th}} = 0$, a smaller peak amplitude will correspond to a pulse with a longer tail, so that, the decay should be positively feedbacked; however, in some cases of $q_{\text{th}} \neq 0$, the smaller peak amplitude may correspond to smaller tails and we expect that the rate decay decreases. We have confirmed this hypothesis as is shown in the simulation results of Fig. 6, where the slope of the curve for peak amplitude decreases with distance. Moreover, taking into consideration that the plasma term will be zero when the optical intensity drops below the threshold intensity, this decay process cannot continue indefinitely. Nevertheless, let us refer that the latter decrease in decay rate was observed even in the presence of additional loss that should have occurred in our simulations due to numerical window limitations.

4 Conclusions

Starting from an evolution equation for pulse propagation in gas-filled PCFs that takes in account group velocity dispersion, Kerr effect and relatively small plasma–light interaction, we used an accelerating variable to find the ODE to which the pulse profiles obey. This ODE has two parameters, the optical intensity threshold for photoionization and one for the plasma nonlinearity strength and acceleration which reduces the effort to compute the profiles and accelerations. We defined two regimes of pulse profile characteristics and propagation. There are symmetrical pulse profiles that are very close to sech and propagate steadily, and asymmetrical pulses presenting a long right tail that shed radiation away as they propagate. The two regimes were identified by two ratios, the peak amplitude over the plasma strength η and the photoionization threshold optical amplitude over η.

Acknowledgments We acknowledge FCT for support through the Projects PTDC/EEA-TEL/105254/2008 (OSP-HNLF), PTDC/FIS/112624/2009 (CONLUZ) and PEst-C/CTM/LA0025/2011.

References

1. J.C. Travers, W. Chang, J. Nold, N.Y. Joly, P.S.J. Russell, J. Opt. Soc. Am. B **28**, A11 (2011)
2. F. Benabid, J.C. Knight, G. Antonopoulos, P.S.J. Russell, Science **298**, 399 (2002)
3. P. Hoelzer, W. Chang, J.C. Travers, A. Nazarkina, J. Nold, N.Y. Joly, M. Saleh, F. Biancalana, P.S.J. Russell, Phys. Rev. Lett **107**, 203901 (2011)
4. M.F. Saleh, W. Chang, P. Hoelzer, A. Nazarkin, J.C. Travers, N.Y. Joly, P.S.J. Russell, F. Biancalana, Phys. Rev. Lett. **107**, 203902 (2011)
5. M.F. Saleh, F. Biancalana, Phys. Rev. A **84**, 063838 (2011)
6. M. Facão, M.I. Carvalho, P. Almeida, Phys. Rev. A **87**, 063803 (2013)
7. D. Wang, Y. Leng, Z. Xu, Appl. Phys. B. Laser Opt. **111**, 447 (2013)
8. M. Facão, D.F. Parker, Phys. Rev. E **68**, 016610 (2003)